10TH INTERNATIONAL SYMPOSIUM ON PARTICLE IMAGE VELOCIMETRY - PIV13
Delft, The Netherlands, July 1-3, 2013

Appropriate spatial filtering of 2D and 3D PIV measurements of wall-bounded turbulent flows

C. Atkinson[1], N.A. Buchmann[1], O. Amili[1] and J. Soria[1,2]

[1] Laboratory for Turbulence Research in Aerospace and Combustion, Department of Mechanical and Aerospace Engineering, Monash University, Victoria, 3800, Australia
Callum.Atkinson@monash.edu

[2] Department of Aeronautical Engineering, King Abdulaziz University, Jeddah, Kingdom of Saudi Arabia

ABSTRACT

Three-dimensional spatial filtering and measurement noise associated with experimental particle image velocimetry (PIV) measurements of wall-bounded flows are investigated via the application of the noiseless transfer function of PIV to the results of direct numerical simulations (DNS) and the comparison with real PIV measurements undertaken at the equivalent spatial resolution. For interrogation region dimensions typical of many PIV experiments the spatial filtering inherent in PIV is shown to significantly underestimate turbulent fluctuations, however in practical experiments this effect is largely offset by measurement noise. In order to determine the noise level and the noise-free effective spatial dynamic range of a given PIV measurement it is therefore necessary to compare experimental measurements in terms of the 1D velocity power spectra and the associated 1D transfer function of PIV, in both the absence of measurement noise and at the equivalent spatial resolution. In this paper the relationship between the 1D transfer function and the 3D transfer function of PIV is explained and a method for identifying the noise dominated scales is demonstrated using data from a tomographic PIV measurement of a turbulent boundary layer. Following this method filtering is applied to reduce the influence of the noise dominated scales and provide experimental PIV velocity fields inline with that which should be generated by a noise free measure of a given spatial dynamic range.

1. INTRODUCTION

Improvement in our understanding of complex fluids flows such as wall-bounded turbulent flows has becoming increasingly dependent on high spatial and temporal resolution direct numerical simulation (DNS), largely driven by their ability to capture the full dynamic range of the flow and the instantaneous three-dimensional velocity and pressure fields. The recent evolution of particle image velocimetry (PIV) based technique into three-dimensional three-component measurements (3C-3D) [1, 2, 3, 4], high-repetition rate time-resolved measurements [5] and the use of multiple high resolution cameras [6] has started to reduced the gap between DNS and experimental measurements, however even planar PIV measurements can still play an important tool in the investigation of turbulent flows. PIV remains particularly relevant at high Reynolds numbers where DNS of the governing equations in not feasible, but also offers critical validation of a range of higher and lower order numerical simulations, whose boundary and inlet conditions or numerical schemes may not necessarily be representative of the true flow physics.

Progress in the study of turbulence requires the complementary use of experiments and numerical simulations in order to overcome their respective limitations. In order to enable the comparison of a given PIV measurement with numerical simulation or theory it is important to be aware of the effects of both spatial filtering and measurement noise and influence of each on the range of scales that are accurately resolved by the measurement. While the theoretical spatial dynamic range (SDR) of a measurement can easily be identified from the ratio of the field of view to twice the interrogation window size, the measurement noise in PIV often out-weights the strength of the true turbulent flow at higher wave-numbers and as such can significantly reduce the range of scales of the flow that are accurately resolved by PIV [7]. In wall-bounded turbulence both seeding density and gradients vary significantly with height above the wall, resulting in a measurement noise levels that can increase from 0.01 pixels in the freestream to greater than 0.1 pixels in the vicinity of a wall, with the possibility of even higher errors in a given experimental measurements due to a combination of image sensor noise, non-uniform particle distributions, laser sheet intensity variations, particle distortions and reflections.

When assessing the accuracy of a given PIV measurement in turbulent flows it is common to find researchers comparing the mean and root mean square velocity profiles or Reynolds stresses with those calculated from often higher resolution hot-wire anemometer (HWA) measurements or DNS [8, 9]. As will be shown in this paper, this comparison can lead to an underestimation of measurement noise due to this noise being offset by the spatial filtering associated with PIV. By not accounting for this spatial filtering PIV measurements can appear to provide a good estimate of the turbulent fluctuations in the flow, while in reality the flow may be spatially under-resolved and largely contaminated by noise.

In this paper we explore the three-dimensional spatial filtering and measurement noise associated with experimental PIV measurements by comparing experimental PIV velocity fields with those obtained by spatially filtering the results from DNS of a zero pressure gradient turbulent boundary layer. The relationship between the analytical 3D transfer function of PIV and the observed 1D transfer function

between the power spectra of the unfiltered and filtered velocity field is explored and a means of identifying the noise dominated wave-numbers and the effective SDR of a PIV measurement is demonstrated using data from a 3D tomographic PIV measurement of a turbulent boundary layer.

2. THE 3D AND 1D TRANSFER FUNCTIONS OF NOISELESS PIV MEASUREMENTS OF WALL-BOUNDED FLOWS

In order to appreciate the influence of spatial resolution on PIV measurements it is instructive to consider the analytical 3D transfer function of PIV in the absence of measurement noise. Details of the derivation of three dimensional transfer function H_{3D} associated with PIV can be found in [10, 11, 12] among others, where if the influence of velocity gradients is neglected and sufficient and uniform seeding and light sheet intensity is assumed, then the velocity measured by PIV is represented by the volume average of the measured velocity from each particle inside the interrogation region such that:

$$H_{3D}(k_x,k_y,k_z) = \frac{\sin(k_x\Delta W_x/2)\sin(k_y\Delta W_y/2)\sin(k_z\Delta W_z/2)\sin(k_xU\Delta t/2)}{(k_x\Delta W_x/2)(k_y\Delta W_y/2)(k_z\Delta W_z/2)(k_xU\Delta t/2)} \tag{1}$$

where k_x,k_y,k_z represents the wave-numbers and $\Delta W_x,\Delta W_y,\Delta W_z$ are the PIV cross-correlation interrogation region dimension in the x,y,z directions, respectively. U is the mean velocity which in the case of zero-pressure gradient wall-bounded flow is entirely longitudinal, enabling the temporal filtering between two laser pulses to be represented in terms of k_x. While the remainder of this paper will focus on 3D velocity fields it is important to note that the transfer function of PIV remains a function of all three wave-number, even in the case of a planar 2D PIV measurements, due to spatial filtering across the light-sheet thickness or the effective depth-of-field of the imaging system.

In the case of a *perfect* or noiseless PIV measurement, where image and cross-correlation measurement noise are negligible, the velocity field that should by return from a PIV measurement of a wall-bounded flow can be determined by applying equation 1 to a higher resolution DNS [13]. In most cases the particle displacement associated with $U\Delta t$ is small enough that the application of the 3D PIV transfer function can be represented by a 3D spatial box-filtering over a domain corresponding to the PIV interrogation window size. While the spatial filtering has little effect on the mean velocity profile, with the exception of the very near wall region (details of which can be found in [12]), the size of the interrogation region has a significant effect on the fluctuating velocity and Reynolds stress profiles as shown in figure 1. Underestimations of the fluctuating velocities in real PIV data are often far smaller than those presented here, the reason for which will be discussed in section 3.

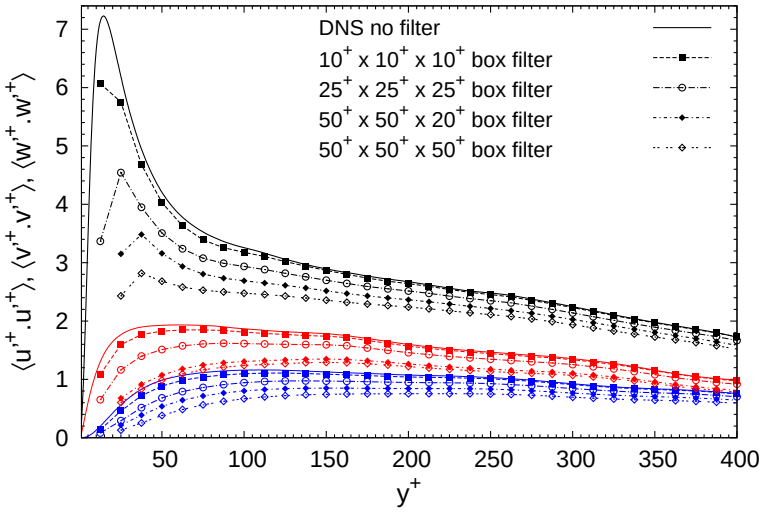


Figure 1: Profiles of Reynolds stresses: $\langle u'.u'\rangle$ (black), $\langle v'.v'\rangle$ (blue) and $\langle w'.w'\rangle$ (red) for unfiltered TBL DNS at $\mathrm{Re}_\theta = 1840$ and noiseless spatial filtered DNS with PIV interrogation regions of $\Delta W_x \times \Delta W_y \times \Delta W_z = 10^+ \times 10^+ \times 10^+$; $25^+ \times 25^+ \times 25^+$; $50^+ \times 50^+ \times 20^+$; and $50^+ \times 50^+ \times 50^+$.

When exploring the range of scales that are resolved by a given measurement and as will be shown later the effect of measurement noise, it is beneficial to consider the 1D longitudinal velocity power spectra (see figure 2). The 1D spectra is considered as it can be readily computed from either DNS, HWA or PIV and demonstrates the attenuation of the measurements at higher wave-numbers as the spatial resolution of the PIV measurement is decreased. In order to compare the 1D spectra of PIV ($E_{11\,PIV}$) and the unfiltered flow or in this case the DNS ($E_{11\,DNS}$) a 1D transfer function can be defined:

$$|H(k_x)|^2 = \frac{E_{11\,PIV}}{E_{11\,DNS}}, \tag{2}$$

which corresponds to the 1D representation of the PIV transfer function $H_{3D}(k_x,k_y,k_z)$. The analytical relationship between these transfer functions is discussed further in [12], but essentially involves a coupling with the true 3D flow spectra and an integration over

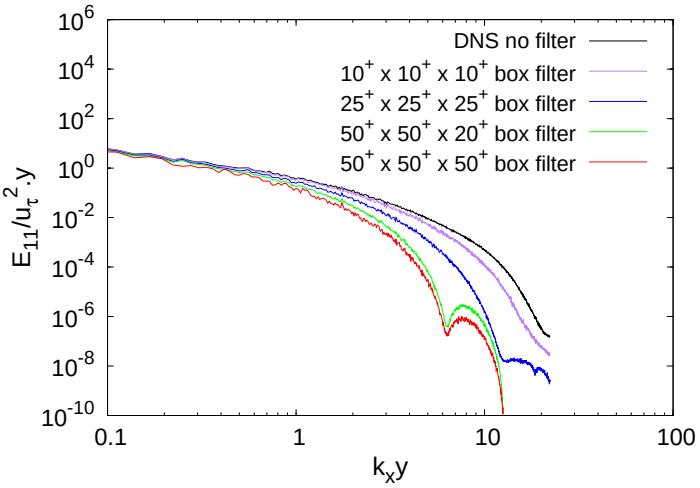


Figure 2: Longitudinal velocity power spectra for unfiltered TBL DNS at $\mathrm{Re}_\theta = 1840$ and spatial filtered DNS with PIV interrogation regions of $\Delta W_x \times \Delta W_y \times \Delta W_z = 10^+ \times 10^+ \times 10^+$, $25^+ \times 25^+ \times 25^+$, $50^+ \times 50^+ \times 20^+$, and $50^+ \times 50^+ \times 50^+$ at wall height $y^+ = 50$

the k_y and k_z wave-numbers as follows:

$$|H(k_x)|^2 = \frac{2\int_{-\infty}^{+\infty}\int \Phi_{ii}(k_x,k_y,k_z)H_{3D}(k_x,k_y,k_z)\,\mathrm{d}k_y\,\mathrm{d}k_z}{2\int_{-\infty}^{+\infty}\int \Phi_{ii}(k_x,k_y,k_z)\,\mathrm{d}k_y\,\mathrm{d}k_z}, \tag{3}$$

where Φ_{ii} is the true 3D spectra of the flow.

The difference between the 3D transfer function along the $(k_x,0,0)$ and the 1D transfer function is demonstrated in figure 3. Given that in the absence of measurement noise PIV essentially represents a low-pass filter, then a -3 dB cut-off wave-number can be defined for PIV as the point at which the spectrum of the PIV measurement is reduced to half the power of the true flow spectrum. In reality the cut-off in the longitudinal wave-number ($\mathrm{k_{c\ 3D}}$) is only a function of the interrogation window length ΔW_x as shown in the 3D transfer function, however by reducing the transfer function to 1D an apparent 1D cut-off ($\mathrm{k_{c\ 1D}}$) is created that can be much lower than the true cut-off. A drop in the amplitude of the transfer function is also observed at even the lowest resolved wave-number ($\mathrm{k_{min}}$) despite these wave-number being unaffected by the true transfer function. The response of a turbulent flow to the spatial filtering inherent in PIV and the differences between the 3D transfer function of PIV and the 1D both play an important role in the determination of the noise-level and noise limited spatial dynamic range.

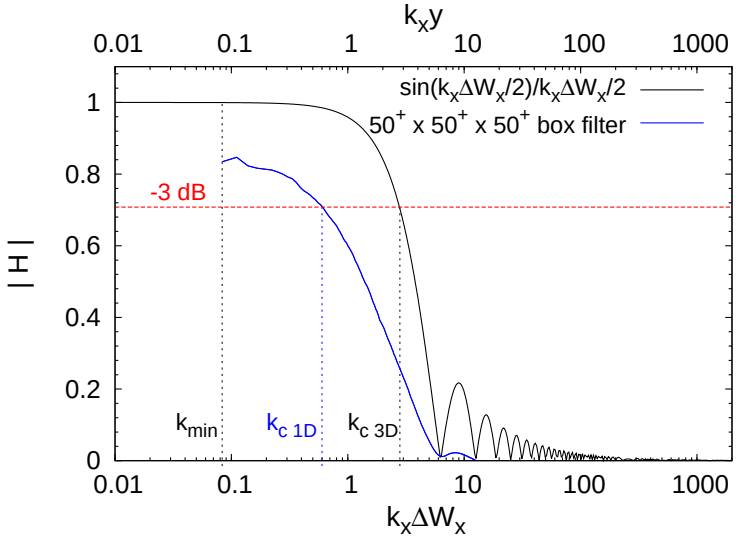


Figure 3: 1D transfer function associated with the longitudinal 1D velocity power spectra for unfiltered TBL DNS at $\mathrm{Re}_\theta = 1840$ and spatial filtered DNS with PIV interrogation regions of $\Delta W_x \times \Delta W_y \times \Delta W_z = 50^+ \times 50^+ \times 50^+$ at wall height $y^+ = 50$.

3. IDENTIFYING THE NOISE LIMITED SDR IN TPIV MEASUREMENTS OF A TURBULENT BOUNDARY LAYER

In order to demonstration the rationale and methodology for determining the noise limited SDR of a practical PIV measurement data from a TPIV measurements of turbulent boundary layer at $\mathrm{Re}_\theta = 7800$ shall be considered, for which the details of the experimental setup and comparative HWA can be found in [14]. A similar yet more detailed demonstration of this methodology for planar PIV measurements of a channel flow can be found in [12]. In this case tomographic reconstruction was performed using 10 iterations of the MLOS-SMART approach [15] with volume dimensions of $1200 \times 180 \times 1200$ points in the longitudinal, wall-normal and spanwise directions, respectively. 3D cross-correlation based PIV analysis was applied with a final interrogation window size of $64 \times 32 \times 64$ pixels, corresponding to viscous units of $26^+ \times 13^+ \times 26^+$.

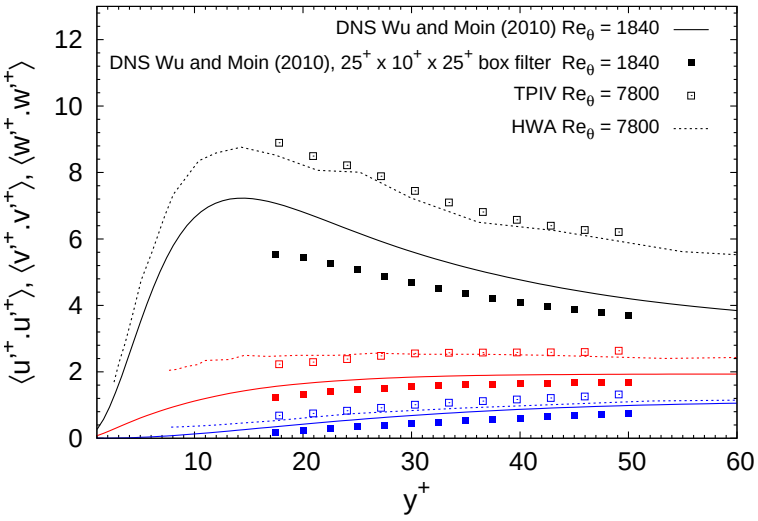


Figure 4: Profiles of Reynolds stresses: $\langle u'.u'\rangle$ (black), $\langle v'.v'\rangle$ (blue) and $\langle w'.w'\rangle$ (red) for TPIV and HWA measurements at $\mathrm{Re}_\theta = 7800$ and the unfiltered DNS at $\mathrm{Re}_\theta = 1840$ and spatial filtered DNS with the equivalent PIV interrogation regions of $\Delta W_x \times \Delta W_y \times \Delta W_z = 25^+ \times 10^+ \times 25^+$ wall units.

Figure 4 shows the difference between the Reynolds stresses measured by TPIV and higher spatial resolution HWA measurements undertaken in the same facility (wire length $\approx 4^+$), along with the lower Reynolds number DNS and spatial filtered DNS with interrogation region dimensions similar to those of the TPIV measurement. In this case the difference in Reynolds numbers between the DNS and HWA results in stronger fluctuations in TPIV, however the effect of the spatial filtering of the TPIV should result in a similar difference between the TPIV and HWA to that observed between the unfiltered and spatially filtered DNS. Instead TPIV overestimates the fluctuations which is indicative of a significant contribution from measurement noise (as identified in [14]). The influence of this noise is clearly seen in the comparison of the longitudinal power spectra (see figure 5), which causes the measured PIV spectra to peal away from the HWA and DNS spectra. In contrast a comparison of only the Reynolds stress profile suggests a relatively accurate measurements of the fluctuations, which would not be possible in the absence of this measurement noise.

Using the comparative velocity spectra in figure 5 a maximum noise limited wave-number k_{max} of the TPIV measurement can be determined as the point where the signal to noise ratio (SNR) between the 1D spectra of the noise in the PIV measurement E_{noise} and the 1D spectra of the real flow $E_{11\ \mathrm{flow}}$ is equal to unity [7]. Foucaut et al. [7] used this methodology to calculate a value of k_{max} as the wave-number where the measured spectra diverged from the true spectra under the 3D transfer function of PIV:

$$E_{11\,PIV}(k\mathrm{max}) = 2E_{11\,flow}(k\mathrm{max}) \left(\frac{\sin k_{\mathrm{max}} \Delta W_x/2}{k_{\mathrm{max}} \Delta W_x/2} \right)^2 \tag{4}$$

This method fails to account for the difference between the 3D transfer and the 1D transfer function, similar to comparing the measured spectra with the true full resolution spectra, rather than the spatially filtered spectra that should be returned in the absence of measurement noise. If the calculated 1D transfer function is applied then a maximum wave-number of k_{maxfilt} is obtained.

$$\begin{aligned} E_{11\,PIV}(k_{\mathrm{maxfilt}}) &= 2E_{11\,flow}(k_{\mathrm{maxfilt}}) \left| H(k_{\mathrm{maxfilt}}) \right|^2 \\ &\approx 2E_{11\,filt}(k_{\mathrm{maxfilt}}) \end{aligned} \tag{5}$$

The inclusion of the calculated 1D transfer function leads to a lower apparent noise limited wave-number, however it is important to note that this represents the 1D wave-number, which as in the case of the cut-off wave-numbers of the 1D and 3D PIV transfer functions, $k_{\mathrm{c\ 1D}}$ and $k_{\mathrm{c\ 3D}}$, is lower than the true 3D noise limited wave-number. Consider the relationship between the 1D and 3D

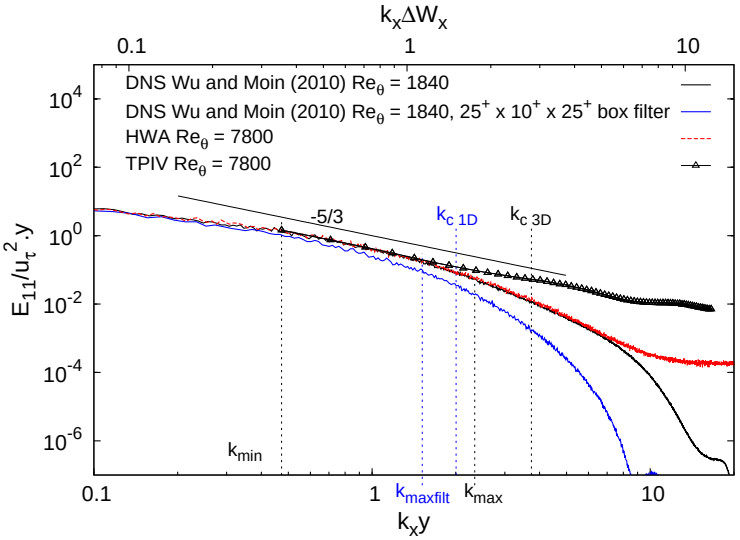


Figure 5: Velocity power spectra at $y^+ = 34$ for TPIV and HWA measurements at $\mathrm{Re}_\theta = 7800$ and the unfiltered DNS at $\mathrm{Re}_\theta = 1840$ and spatial filtered DNS with the equivalent PIV interrogation regions of $\Delta W_x \times \Delta W_y \times \Delta W_z = 25^+ \times 10^+ \times 25^+$ wall units.

transfer function of a 3D Gaussian filter that might be used to filter the signal at the noise dominated wave-numbers:

$$|H_{filt}(k_x)|^2 = \frac{2\int_{-\infty}^{+\infty}\int \Phi_{PIV\,11}(k_x,k_y,k_z)H_{filt\,3D}(k_x,k_y,k_z)\,\mathrm{d}k_y\,\mathrm{d}k_z}{2\int_{-\infty}^{+\infty}\int \Phi_{PIV\,11}(k_x,k_y,k_z)\,\mathrm{d}k_y\,\mathrm{d}k_z}, \tag{6}$$

Note that this transfer function depends on the noise effected 3D measurement spectrum and is therefore not necessarily the same as that of equation 2. When applied to the TPIV velocity field (see figure 6) a $3 \times 3 \times 3$ point Gaussian filter provided a similar 1D cut-off wave-number to k_{maxfilt} with an apparent 1D cut-off of $k_{c\,1D}.y = 1.9$ for the present case. In terms of the true 3D wave-number space this corresponds to a 3D cut-off $k_{c\,3D}.y = 4.5$, which it turns out is actually higher than the k_{max} determined from the use of the 3D transfer function in equation 4. Despite a small variation in the 1D cut-off of the filter and the maximum 1D noise-limited wave-number, the use of this filter provides a similar drop in the 1D spectra and Reynolds stress, in line with what should be expected from a noiseless TPIV measurement.

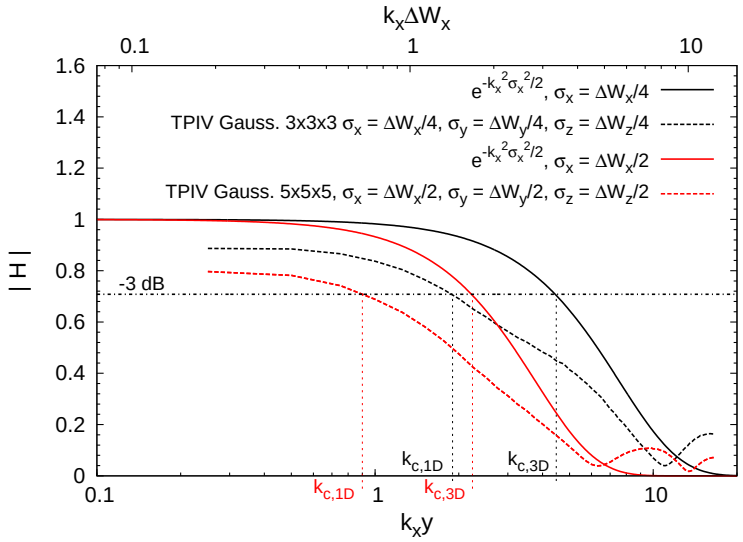


Figure 6: Difference between apparent 1D transfer function associated with the 3D Gaussian filtering of the TPIV data at $\mathrm{Re}_\theta = 7800$ and $y^+ = 34$ with interrogation regions of $\Delta W_x \times \Delta W_y \times \Delta W_z = 26^+ \times 12^+ \times 26^+$ wall units.

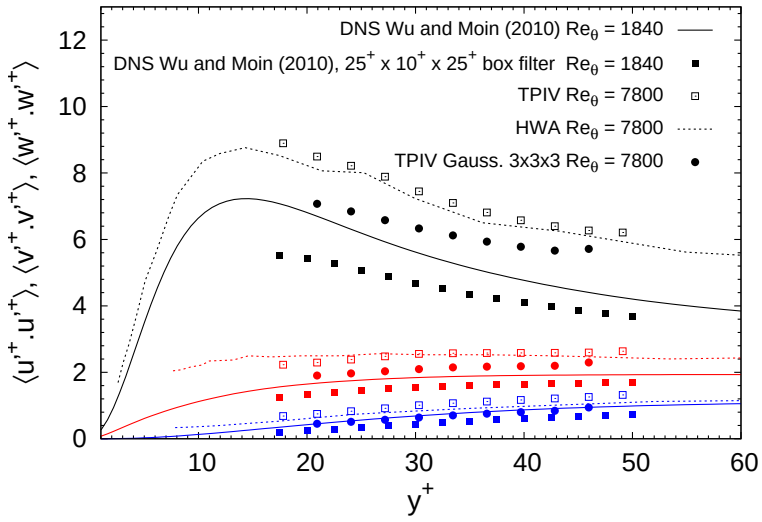


Figure 7: Profiles of Reynolds stresses $\langle u'.u'\rangle$, $\langle v'.v'\rangle$ and $\langle w'.w'\rangle$ for raw and $3\times3\times3$ Gaussian filtered TPIV and HWA measurements at $\mathrm{Re}_\theta = 7800$ and the unfiltered DNS at $\mathrm{Re}_\theta = 1840$ and spatial filtered DNS with the equivalent PIV interrogation regions of $25^+\times10^+\times25^+$ wall units.

4. CONCLUSION

The effects of three-dimensional spatial filtering and the measurement noise associated with experimental PIV measurements of wall-bounded turbulent flows are investigated by comparing the transfer function of noiseless PIV with the results of a practical TPIV experiment. Noiseless PIV measurements are shown to significantly underestimate velocity fluctuations and Reynolds stresses. In real experiments measurement noise offsets this effect resulting in a measurement that may appears to provide a good estimate of the turbulent fluctuations in the flow, when in reality the true turbulent fluctuations are under-resolved and supplemented by measurement noise. A means of determining the noise level in a given measurement is presented based on the 1D velocity power spectra and the incorporation of the apparent 1D transfer function of PIV. The difference between the 1D and 3D transfer function is explored and if not taken in to account can result in an underestimation of the maximum resolved wave-number by as much as 50%. By combining this approach with an appropriate spatial filter it is possible to remove the noise dominated small scales and estimate the effective spatial dynamic range of a PIV measurement, as required for appropriate comparison with numerical results and theory.

ACKNOWLEDGMENTS

The support of Australian Research Council for this work is gratefully acknowledged. TPIV experiments were perform in collaboration with researchers at the Laboratoire de Mécanique de Lille, during which time C.A. was supported by an Eiffel Fellowship and an Australian Postgraduate Award. Our thanks to Associate Professor Xiaohua Wu for graciously providing the DNS velocity fields that were used in this study.

REFERENCES

[1] Ellenrieder, K. V. and Soria, J. (2003) Experimental measurements of particle depth of field in digital holography. *International Workshop on holographic metrology in fluid mechanics*, Loughborough University, May.

[2] Meng, H., Pan, G., Pu, Y., and Woodward, S. H. (2004) Holographic particle image velocimetry: from film to digital recording. *Measurement Science and Technology*, **15**, 673–685.

[3] Elsinga, G. E., Scarano, F., Wieneke, B., and Oudheusden, B. W. v. (2006) Tomographic particle image velocimetry. *Experiments in Fluids*, **41**, 933–947.

[4] Soria, J. and Atkinson, C. (2008) Towards 3C-3D digital holographic fluid velocity vector field measurement - tomographic digital holographic PIV (tomo-HPIV). *Measurement Science and Technology*, **19**, 1–12.

[5] Baur, T. and Koengeter, J. (2000) High-speed PIV and the post-processing of time-series results. *Euromech 411*.

[6] Herpin, S., Wong, C. Y., Stanislas, M., and Soria, J. (2008) Stereoscopic PIV measurements of a turbulent boundary layer with a large spatial dynamic range. *Experiments in Fluids*, **45**, 745–763.

[7] Foucaut, J. M., Carlier, J., and Stanislas, M. (2004) Piv optimization for the study of turbulent flow using spectral analysis. *Measurement Science and Technology*, **15**, 1046–1058.

[8] Carlier, J. and Stanislas, M. (2005) Experimental study of eddy structures in a turbulent boundary layer using particle image velocimetry. *J. Fluid Mech.*, **535**, 143–188.

[9] Ganapathisubramani, B., Hutchins, N., Hambleton, W. T., Longmire, E. K., and Marusic, I. (2005) Investigation of large-scale coherence in a turbulent boundary layer using two-point correlations. *J. Fluid Mech.*, **524**, 57–80.

[10] Lourenco, L. and Krothapalli, A. (2000) True resolution PIV, a mesh free second order accurate algorithm. *Proc. 10th Int. Symp. Appl. Laser Tech. Fluid Mech.*, Lisbon, Portugal.

[11] Lavoie, P., Avallone, G., De Gregorio, F., Romano, G. P., and Antonia, R. A. (2007) Spatial resolution of PIV for the measurement of turbulence. *Experiments in Fluids*, **43**, 39–51.

[12] Atkinson, C., N. A. Buchmann, O. A., and Soria, J. (2013) On the appropriate filtering of piv measurements of turbulent shear flows. *Exp. Fluids*, **submitted**.

[13] Wu, X. and Moin, P. (2010) Transitional and turbulent boundary layer with heat transfer. *Phys. Fluids*, **22**.

[14] Atkinson, C., Coudert, S., Foucaut, J.-M., Stanislas, M., and Soria, J. (2011) The accuracy of tomographic particle image velocimetry for measurements of a turbulent boundary layer. *Experiments in Fluids*, **50**, 1031–1056, 10.1007/s00348-010-1004-z.

[15] Atkinson, C. and Soria, J. (2009) An efficient simultaneous reconstruction technique for tomographic particle image velocimetry. *Experiments in Fluids*, **47**, 553–568.